

## Chemical Sensing Based on Catalytic Nanomotors: Motion-Based Detection of Trace Silver

Daniel Kagan,<sup>†</sup> Percy Calvo-Marzal,<sup>†</sup> Shankar Balasubramanian,<sup>†</sup> Sirilak Sattayasamitsathit,<sup>†</sup>  
Kalayil Manian Manesh,<sup>†</sup> Gerd-Uwe Flechsig,<sup>‡</sup> and Joseph Wang<sup>\*,†</sup>

Department of Nanoengineering, University of California San Diego, La Jolla, California 92093, and Department of Chemistry, University of Rostock, D-18051 Rostock, Germany

Received June 22, 2009; E-mail: josephwang@ucsd.edu

Considerable recent efforts have been devoted to the development of artificial nanomotors.<sup>1</sup> In particular, fuel-driven bisegment Au–Pt nanowires exhibit autonomous self-propulsion due to electrocatalytic decomposition of hydrogen peroxide fuel.<sup>1,2</sup> Such autonomous motion of catalytic nanowire motors holds great promise for exciting applications ranging from drug delivery, nanoscale assembly and transport, or motion-based biosensing.<sup>1</sup>

This communication reports on the first example of using catalytic nanomotors for motion-based chemical sensing, and particularly for specific detection of trace silver ions. During recent experiments in our laboratory involving electrochemically triggered motion of catalytic nanowire motors,<sup>3</sup> we observed unusual speed acceleration associated with silver ions generated at a pseudo silver-wire reference electrode placed in the vicinity of the nanowire motors. Such an unexpected specific silver effect upon the speed of catalytic nanomotors has been exploited in the present work for designing a new motion-based silver sensing protocol. The new protocol relies on the use of an optical microscope for tracking the speed of nanowire motors and offers highly selective, sensitive, and simple measurements of trace silver based on direct visualization.

Figure 1A displays traces of Au–Pt nanomotors (over a 3 s period), taken from videos of the nanowires in the presence of 11 different cations (100  $\mu\text{M}$  each), along with the peroxide fuel. Of these cations, 10 caused a significant speed reduction, including a Brownian motion or a slower non-Brownian motion (with speeds ranging from 0.3 to 7.1  $\mu\text{m s}^{-1}$ ). Such slow speed (compared to an actual speed of  $\sim 10 \mu\text{m s}^{-1}$  observed without these salts) is consistent with the self-electrophoresis mechanism for the propulsion of catalytic nanomotors,<sup>4</sup> where the speed decreases linearly with the solution conductivity.<sup>5</sup> In contrast, the nanomotors move over a dramatically longer path in the presence of silver (shown in the middle), displaying an average speed of 52  $\mu\text{m s}^{-1}$ . Also shown in Figure 1B is the histogram depicting the average speed of the nanomotors in the presence of the different cations tested. These data, along with the corresponding video (shown in the Supporting Information; SI Video 1), clearly illustrate the remarkably selective acceleration in the presence of silver. Adding other cations (e.g.,  $\text{Pb}^{2+}$  or  $\text{K}^+$  up to 5  $\mu\text{M}$ ) had only slight reductions in the speed signal in the presence of the silver analyte. Apparently, the presence of a silver ion can greatly minimize the ionic-strength limitation of catalytic nanomotors. A high speed of  $\sim 20 \mu\text{m s}^{-1}$  was maintained in the presence of 0.1 mM  $\text{K}^+$  (compared to a slower motion of 7  $\mu\text{m s}^{-1}$  observed for  $\text{K}^+$  without the silver). Higher (>mM) salt concentrations, however, led to the expected conductivity-induced speed diminution.

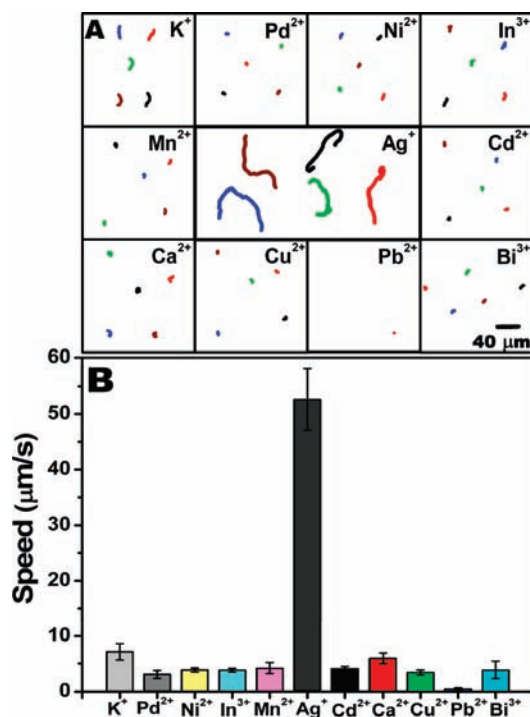


**Figure 1.** Motion of Au–Pt catalytic nanomotors in a 5%  $\text{H}_2\text{O}_2$  solution containing 11 common cations. (A) Image displaying 3 s track lines for the movement of 5 randomly selected nanomotors in 11 different 100  $\mu\text{M}$  metal–nitrate salt solutions (of  $\text{K}^+$ ,  $\text{Pd}^{2+}$ ,  $\text{Ni}^{2+}$ ,  $\text{In}^{3+}$ ,  $\text{Mn}^{2+}$ ,  $\text{Ag}^+$ ,  $\text{Cd}^{2+}$ ,  $\text{Ca}^{2+}$ ,  $\text{Cu}^{2+}$ ,  $\text{Pb}^{2+}$ , and  $\text{Bi}^{3+}$ ). (B) Corresponding bar graph comparing the average nanomotor speed (conditions same as those in A). Error bars for  $n = 20$ .

The highly selective motion-based response is characterized also with a defined concentration dependence, with the speed (or distance) providing the quantitative information. Figure 2A–D display track lines of the catalytic nanomotors (over a 2 s period) obtained in the presence of different silver concentrations (0, 1, 10, and 100  $\mu\text{M}$ ; A–D). These traces indicate clearly that the nanomotors travel longer distances (ranging from 19 to 104  $\mu\text{m}$ ) upon increasing the silver concentration. Such paths correspond to speeds ranging from 9.6  $\mu\text{m s}^{-1}$  (without silver) to 52  $\mu\text{m s}^{-1}$  (at 100  $\mu\text{M}$  silver). Also shown in Figure 2E is a calibration plot of the speed vs silver concentration over the  $10^{-9}$  to  $10^{-4}$  M range. Such a plot displays a defined concentration dependence over the 0.5 to 100  $\mu\text{M}$  range, along with a negligible concentration effect at lower Ag(I) levels. The well-defined concentration dependence is clearly illustrated from the corresponding videos (shown in SI Video 2). Note that the behavior observed in Figure 2 is conflicting to what is commonly expected upon increasing the salt concentration.<sup>5</sup>

<sup>†</sup> University of California San Diego.

<sup>‡</sup> University of Rostock.

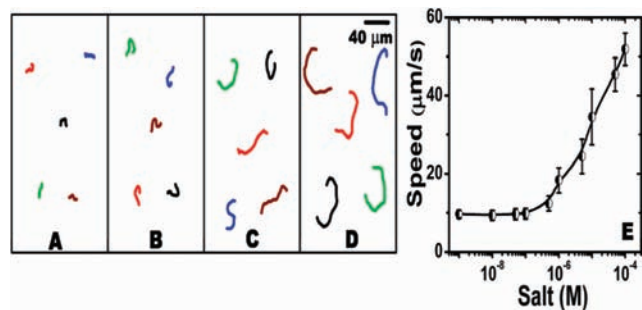


**Figure 2.** Track lines of nanomotors illustrating the distances traveled by five Au–Pt nanowires in the presence of different Ag(I) concentrations: 0 (A), 1 (B), 10 (C), and 100 (D)  $\mu\text{M}$ , along with 5 wt %  $\text{H}_2\text{O}_2$  fuel solution. (E) A calibration curve for Ag(I) over the micromolar range (0.5–100  $\mu\text{M}$ ). Other conditions same as those in Figure 1.

Several possible mechanisms have been considered to explain the unusual acceleration of Au–Pt nanomotors in the presence of silver ions. The most promising explanation relies on the underpotential deposition (UPD) of silver on the Au–Pt nanowires. With the addition of silver ions, these ions adsorb over the nanowire surface and are then reduced in the presence of hydrogen peroxide. Energy dispersive X-ray spectroscopy (EDX) measurements confirmed the presence of metallic silver over the Pt and Au segments of the nanowires (at 13 and 0.4 Ag atomic %, respectively), following a 0.5 h exposure to the silver nitrate/hydrogen peroxide solution. A clear change of the color of the Pt segment was observed from analogous SEM experiments. No such compositional or color changes were observed in the presence of silver alone (without hydrogen peroxide). As will be illustrated below, a similar silver deposition was observed on platinum and gold nanorods. In addition, nanomotors exposed to a 100  $\mu\text{M}$  Ag(I)/5%  $\text{H}_2\text{O}_2$  solution for 0.5 and 24 h, followed by a thorough wash with nanopure water, displayed high speeds of 20 and 35  $\mu\text{m s}^{-1}$ , respectively, in a fresh silver-free 5%  $\text{H}_2\text{O}_2$  solution. These data confirm that the deposited Ag(0), rather than the dissolved Ag(I), is responsible for the accelerated motion. The possibility of depositing Ag(0) by UPD onto gold nanorods and platinum surfaces was discussed by several groups.<sup>6</sup>

Such silver deposition onto catalytic nanowires can lead to differences in the surface and catalytic properties (and hence to a faster axial speed). Deposition of silver onto the Au segment increases the mixed potential difference ( $\Delta E$ ) between the anodic and cathodic segments, leading to an accelerated nanomotor motion in a manner similar to that reported recently for high-speed alloy nanomotors.<sup>7</sup> Similarly, the silver deposition onto the Pt segment may make it more catalytically active. The accelerated electrocatalytic decomposition of hydrogen peroxide was indicated also by the sharp decline of the motor speed following a 10 min exposure to the silver ion (compared to a longer  $\sim 30$  min period observed without silver). The faster speed was then restored upon restoring the initial fuel level.

To isolate the role of the individual segments upon speed acceleration, the motility of monocomponent Pt and Au nanorods was examined in the presence of silver nitrate. Surprisingly, monocomponent Pt rods displayed a dramatic acceleration from 3.5 to 22.6  $\mu\text{m s}^{-1}$  in the presence of 10  $\mu\text{M}$  silver ion (SI Video 3). Monocomponent Au nanorods, in contrast, display a Brownian motion in the presence and absence of Ag(I). The EDX data of SI Figure 1 confirm the presence of silver on monocomponent Pt and Au nanowires, with Ag(0) values of up to 18 and 10 (Ag atomic %), respectively. Apparently, the Ag(0) deposition onto monocom-

ponent platinum nanowires leads to the asymmetry (bimetal character) essential to induce the electrocatalytic propulsion. This is in agreement with a recent hydrogen peroxide based fuel cell study where a Pt–Ag (anode–cathode) combination exhibits the highest current density compared to other anode–cathode combinations, including Au–Ag.<sup>8</sup> Similarly, it was reported that Au–Ag bimetallic nanowire motors have a very slow speed of 6  $\mu\text{m s}^{-1}$ .<sup>4</sup> The self-diffusiophoresis mechanism<sup>9</sup> may also be considered for explaining the silver effect. Here, the deposition of silver over the nanomotors increases the localized gradient of reaction products around the nanomotors, leading to a diffusiophoretic movement of the nanomotor.<sup>9</sup> Such an ionic gradient around the nanomotors results in a net electric field in solution that facilitates the increased speed.

In summary, we have described the first example of motion-based chemical sensing involving fuel-driven nanomotors. Effective measurements of trace Ag(I) have been accomplished based on the dramatic and specific acceleration of bimetal nanowire motors in the presence of this ion. While these initial data clearly demonstrate the utility of catalytic nanomotors for measuring micromolar concentrations of silver, additional work is required toward a better understanding of the unusual silver effect or the defined concentration dependence and for adapting the new concept for practical real-life applications. The presence of silver also facilitates the operation of catalytic nanomotors in conducting media that were not accessible earlier to catalytic nanomotors. While the new concept of motion-based sensing has been illustrated for trace measurements of Ag(I), we anticipate that it would lead to a wide range of novel sensing protocols. Current efforts in our laboratory examine new bioaffinity displacement assays based on the ability of a target biomolecule to trigger the movement of an anchored nanomotor. We expect that such motion-based bioassays would lead to remarkable sensitivity, reflecting the ability to detect single-binding events.

**Acknowledgment.** This work was supported by NSF (Award Number CHE 0840684) and NIH (Award RO1 EB002189). G.U.F. thanks the Deutsche Forschungsgemeinschaft for a Heisenberg fellowship FL 384/7-1.

**Supporting Information Available:** Related protocols, instrumentation, reagents, additional data, and videos. This material is available free of charge via the Internet at <http://pubs.acs.org>.

## References

- (a) Kline, T. R.; Paxton, W. F.; Mallouk, T. E.; Sen, A. *Angew. Chem., Int. Ed.* **2005**, *44*, 744. (b) Wang, J. *ACS Nano* **2009**, *3*, 4. (c) Ozin, G. A.; Manners, I.; Fournier-Bidoz, S.; Arsenaault, A. *Adv. Mater.* **2005**, *17*, 3011.
- (a) Paxton, W. F.; Sen, A.; Mallouk, T. E. *Chem. Eur. J.* **2005**, *11*, 6462. (b) Burdick, J.; Laocharoensuk, R.; Wheat, P. M.; Posner, J. D.; Wang, J. *J. Am. Chem. Soc.* **2008**, *130*, 8164.
- Calvo-Marzal, P.; Manesh, K. M.; Kagan, D.; Balasubramanian, S.; Cardona, M.; Flechsig, G.-U.; Posner, J.; Wang, J. *Chem. Commun.* **2009**, 4509.
- Wang, Y.; Hernandez, R. M.; Bartlett, D. J.; Bingham, J. M.; Kline, T. R.; Sen, A.; Mallouk, T. E. *Langmuir* **2006**, *22*, 10451.
- Paxton, W. F.; Baker, P. T.; Kline, T. R.; Wang, Y.; Mallouk, T. E.; Sen, A. *J. Am. Chem. Soc.* **2006**, *128*, 14881.
- (a) Mascaro, L. H.; Santos, M. C.; Machado, S. A. S.; Avaca, L. A. *J. Chem. Soc., Faraday Trans.* **1997**, *93*, 3999. (b) Orendorff, C. J.; Murphy, C. J. *J. Phys. Chem. B* **2006**, *110*, 3990. (c) Niidome, Y.; Nakamura, Y.; Honda, K.; Akiyama, Y.; Nishioka, K.; Kawasaki, H.; Nakashima, N. *Chem. Commun.* **2009**, 1754.
- Demirok, U. K.; Laocharoensuk, R.; Manesh, K. M.; Wang, J. *Angew. Chem., Int. Ed.* **2008**, *47*, 9349.
- Yamazaki, S.; Siroma, Z.; Senoh, H.; Ioroi, T.; Fujiwara, N.; Yasuda, K. *J. Power Sources* **2008**, *178*, 20.
- (a) Ibele, M.; Mallouk, T. E.; Sen, A. *Angew. Chem., Int. Ed.* **2009**, *48*, 1. (b) Anderson, J. *Annu. Rev. Fluid Mech.* **1989**, *21*, 61. (c) Howse, J. R.; Jones, R. A. L.; Ryan, A. J.; Gough, T.; Vafabakhsh, R.; Golestanian, R. *Phys. Rev. Lett.* **2007**, *99*, 048102.

JA905142Q